Effect of magnetic field on natural convection inside a partially-heated vertical duct: Experimental study

EFFECT OF MAGNETIC FIELD ON NATURAL CONVECTION INSIDE A PARTIALLY-HEATED VERTICAL DUCT: EXPERIMENTAL STUDY

Masayuki Kaneda*, Kensuke Nazato, Hiroaki Fujiwara, Kengo Wada, Kazuhiko Suga

Department of Mechanical Engineering, Osaka Prefecture University, Sakai 599-8531, Japan

*mkaneda@me.osakafu-u.ac.jp

ABSTRACT

We experimentally study the effect of the magnetic force from one or more block magnets on natural convection of paramagnetic liquid inside a partially-heated duct. The permanent magnet(s) is/are placed partially/fully behind the heated wall. For a single magnet, the local heat transfer coefficient is suppressed near the bottom edge of the magnet and enhanced near the top edge if the magnet edge is behind the heated wall. This effect depends on the elevation of the magnet relative to the heated wall. Using two block magnets with alternating magnetic poles enhances the force and corresponding effect at their junction because of an increase in magnetic flux density.

KEYWORDS: Magnetic force, Heat transfer enhancement, Natural convection, Paramagnetic liquid, Magnetic field

1. INTRODUCTION

Every material has magnetism, and its magnitude is represented by the magnetic susceptibility. Iron, cobalt, and nickel have large positive magnetic susceptibility, and they are categorized as ferromagnetic materials. Other materials have considerably smaller magnetic susceptibility. Materials with small positive susceptibility are called paramagnetic (such as oxygen), and those with small negative susceptibility are diamagnetic (such as water). Although magnetic force on paramagnetic and diamagnetic materials has been reported [1], the force is negligibly weak. Thus, studies are limited to such cases as oxygen gas sensors [2], convection of oxygen [3], and separation of red blood cells from whole blood [4].

Since magnets with magnetic fields of several tesla have become available, new studies have been reported such as on the orientation of carbon nanotubes [5], effects on the evaporation rate of water [6], effects on water, air, and powders [7], and nitrogen jets (Wakayama jets) [8].

In an inhomogeneous magnetic field, the magnetic force on a unit volume $\mathbf{F_m}$ is defined as [9]

$$\mathbf{F_m} = \frac{1}{2}\mu_0\chi_{vm}\nabla\mathbf{H}^2 = \frac{1}{2}\mu_0\rho\chi_{mm}\nabla\mathbf{H}^2 = \frac{\rho\chi_{mm}}{2\mu_0}\nabla\mathbf{B}^2 \quad , \tag{1}$$

where μ_0 is the magnetic permeability in vacuum, $\chi_{vm} = \rho\chi_{mm}$ is the volumetric magnetic susceptibility (with χ_{mm} being the mass magnetic susceptibility and ρ the density), and $\mathbf{H} = \mathbf{B}/\mu_0$ is the magnetic field. The fact that the magnetic force depends on the magnetic susceptibility and the gradient of the squared magnetic induction ($\nabla\mathbf{B}^2$) suggests that differences in magnetic susceptibility among multiple materials can induce some of the aforementioned phenomena [7, 8].

The mass magnetic susceptibility χ_{mm} of the paramagnetic fluid also depends on the inverse of absolute temperature, which is Curie's law,

$$\chi_{mm} = \frac{C}{T} \quad , \tag{2}$$

where C is a constant. This suggests that a low-temperature fluid undergoes a stronger attracting force than a high-temperature fluid. Therefore, magnetic force on paramagnetic fluids has been studied for convection control [3, 10-18]. The magnetic effect can be enhanced by putting the convection system inside a region with large $\nabla\mathbf{H}^2$ ($=\nabla\mathbf{B}^2$). Therefore, the aforementioned studies have been conducted between magnetic poles or inside the bore of a superconducting magnet. Furthermore, the effective space is limited, thus most of these studies tend to use small closed systems. However, a strong superconducting magnet is expensive, thus its use for convection control is limited to such cases as material processing of expensive crystals [19] and convection in extreme conditions such as zero gravity [12].

To extend application, two problems should be solved. One is the cost of strong magnets, and the other is the lack of knowledge of magnetic effects on heat transfer. Therefore, we use the natural convection inside a vertical duct of which one sidewall is partially heated. This phenomenon is seen in fin-bundled heat exchangers, heatsinks, and solar water heaters. Since the natural convection depends on the heat flux and working fluid, an external force may be effective in enhancing the overall heat transfer. To our knowledge, the effect on natural convection in such case has not been studied yet.

Because superconducting magnets are still expensive, using a permanent magnet to enhance/suppress natural convection would reduce the cost of applying a magnetic field. However, since the magnetic induction of a single magnet is limited, the arrangement of magnets is crucial. Electric motors and mag-lev devices have unique magnet arrangements to obtain the effective force of permanent magnets.

Therefore, we experimentally study the natural convection of paramagnetic liquid inside a partially-heated vertical duct in a magnetic field. A single permanent magnet is firstly used to explain and clarify its effects. We numerically predict the magnetic field from the single permanent magnet to explain the effect of the field on the flow. Next, experiments with multiple magnets are conducted to increase the enhancement/suppression of heat transfer, and the effect is discussed in light of the numerically obtained field.

2. EXPERIMENTAL

The experimental procedure consisted of measuring the magnetic susceptibility of the working fluid, estimating heat loss, measuring temperature along the vertical heated plate with a single block magnet, and replacing the single magnet with multiple-magnet arrangements.

2.1 Experimental Setup

The schematic of the experiment is shown in **Fig. 1(a)**. The experimental setup consisted of a vertical duct (**Fig. 1(b)**, vertical heated plate on an acrylic slab with side walls), submerged in a tank with dimensions 320 mm × 220 mm × 720 mm, a DC power supply (Kikusui, PAK35-10A), a thermostatic bath (HAAKE, K20), and a PC with a data logger (Keyence, NR-500 + NR-TH08×2). The tank was filled with aqueous gadolinium nitrate solution as a working fluid at a concentration of approximately 15 wt.%, and the fluid temperature was kept constant at 292 K by the heat exchanger tube connected to the thermostatic bath. The heater bundled in the duct was made of a nonmagnetic stainless foil of dimensions 50 mm × 110 mm × 0.025 mm and was connected to the DC power supply. Since the working fluid would be decomposed by an electric current, the stainless foil could not be soaked in the fluid. To insulate electrically and make the heater as thin as possible to place the magnet closely behind the heater, the foil was laminated by 100 μm-thick EVA coated PET films. For single lamination, the heater would be easily deflected and flatness would not be guaranteed. Therefore, the lamination was repeated three times. The thickness of the heated wall was 0.625 mm. The margin of the laminated film over the stainless foil was 30 mm at the top and 20 mm at the bottom. T-type thin thermocouples were attached just behind the laminated heater along the vertical symmetrical centerline. The elevation of each thermocouple was decided at every experimental run so that the effect of the magnetic field could be measured precisely. Additionally, two thermocouples were put on opposite sides of the heater unit to estimate its heat loss. To prevent flow disturbance from outside of the vertical heated plate [22], side walls and a facing wall (shown in **Fig. 1(b)**) were attached to the heater unit. Therefore, the natural convection is induced inside the confined vertical duct.

In the experiment, $x = 0$ mm corresponded to the starting point of wall heating and x_{mag} was the elevation of the bottom magnet edge, which are indicated in **Fig. 1(b)**.
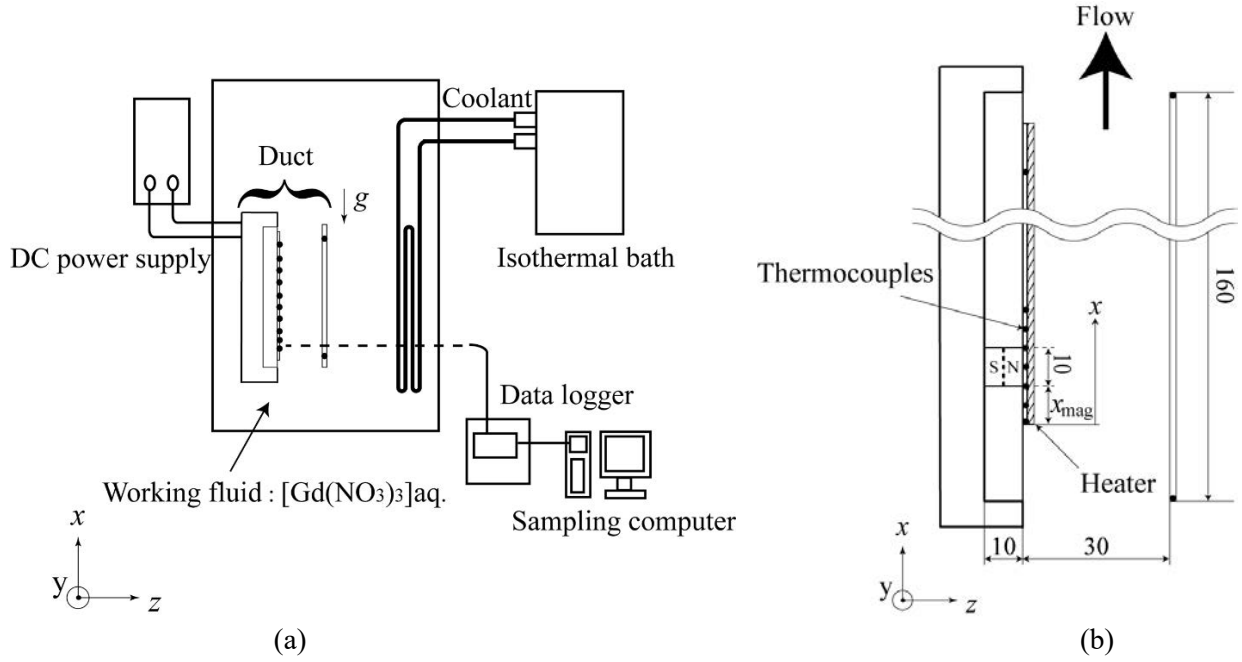
Fig. 1 (a) Schematic of the experimental setup. (b) Enlarged image of the cross section of the duct.

2.2 Working Fluid

Prior to the natural convection experiment, the magnetic susceptibility of the aqueous gadolinium nitrate was measured by using a magnetic balance (Sherwood, MSB-Mk1) at a temperature of 292 K. The measured magnetic susceptibility was 1.205×10^{-7} m³/kg, which agreed with measurements by Maki et al. [15] and Kenjereš et al. [14].

2.3 Procedure

Prior to measuring heat transfer, the heat loss from the heater unit was evaluated by the modified method of Ozoe and Churchill [20]. The duct was rotated 90° so that the heated wall was horizontally above, and the facing wall, which was kept at constant temperature, was below. When the open ends (left and right) were thermally insulated, a thermally conductive state was attained in the working fluid inside the enclosed region (between the heater and facing wall). The heat loss was estimated as the total heat supplied from the heater minus the conduction heat estimated by Fourier's law. The thermal conductivity of the working fluid was taken from Ref. [14].

After the heat loss was estimated, the duct was returned to vertical as shown in **Fig. 1 (b)** and the experiments on natural convection were carried out. For each experimental run, 8 hours were spent to attain steady-state convection and the sampling data were acquired for 1 hour.

After the acquisition, the local heat transfer coefficient h_x W/(m²K) was estimated at each thermocouple location. Its definition is

$$h_x = \frac{q}{T_w - T_\infty} \quad ,$$
(17)

where q is the net heat flux from the heater to the fluid, T_w is the time-averaged local wall temperature measured by thermocouples, and T_∞ is the bulk temperature in the bath. It is better to use the local bulk temperature (mixed mean temperature) at the same elevation where the wall temperature is measured, however, we used the bath bulk temperature for convenience [21].

The local Nusselt and modified Rayleigh numbers were estimated, respectively, by the equations

$$Nu_x = \frac{h_x x}{\lambda} \tag{17}$$

and

$$Ra_x{}^* = \frac{g\beta q x^4}{\alpha \nu \lambda} . \tag{18}$$

The characteristic length x in Nu_x and $Ra_x{}^*$ was defined as the distance from the bottom edge of the heater.

2.4 Experimental Conditions

Throughout the experiments, we fixed $q = 1.25 \, \text{kW/m}^2$ and $T_\infty = 292\text{K}$. We conducted experiments both without a magnetic field and with two magnet arrangements. The size of a single magnet was 10 mm × 40 mm × 10 mm. The first arrangement was a single block magnet to observe the relationship between the magnetic field and resultant effect. Then, to enhance the effect, multiple magnets were used such that each pair of magnets had poles alternately arranged. We observed the effect of magnetic elevation in all cases. The schematic for multiple magnets is presented in the next section.

2.5 Magnetic Field

To discuss the magnetic force on the fluid, it is essential to visualize the magnetic field. We used the free software FEMM (http://www.femm.info/wiki/Documentation/) to solve the Maxwell equations in two dimensions. The magnetic field in the experiment could be regarded as two-dimensional since the magnets were long enough in the spanwise direction. We firstly obtained the magnetic field from a single block magnet (**Fig. 2(a)**) and then that from the multiple-magnet arrangement. **Fig. 2(b)** shows an arrangement of two magnets. In this case, different magnetic poles are alternately aligned, which is employed to health appliances and research study [23]. As in the definition of magnetic force, $\nabla \mathbf{B}^2$ in Eq. (1) is an important component. We expected aligning poles alternately to enhance $\nabla \mathbf{B}^2$ because of the increased magnetic field density. In the simulation, the size of the magnet corresponded to that in the experiment. The permeability was set to $1.26 \times 10^{-6} \, \text{mkg/(s}^2\text{A}^2)$ (air) and $1.32 \times 10^{-6} \, \text{mkg/(s}^2\text{A}^2)$ (Nd-Fe-B magnet with 40 MGOe), and the Robin condition was applied at the boundary in the computational domain (mixed boundary condition).
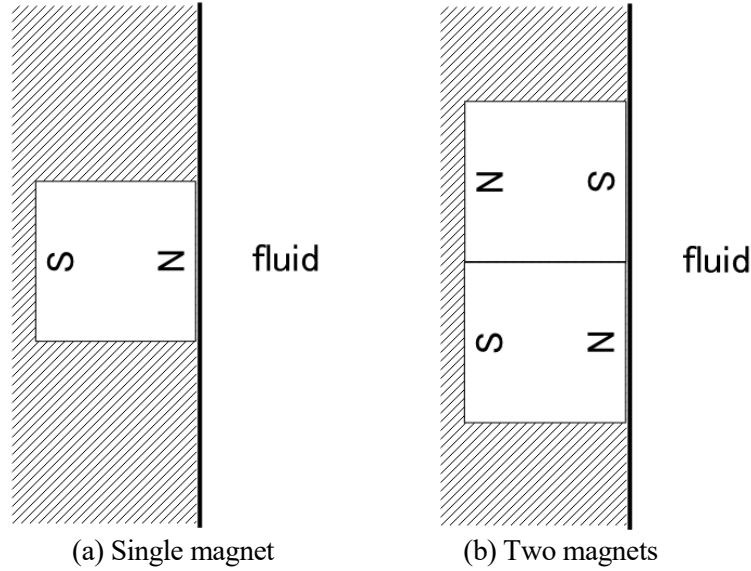
(a) Single magnet   (b) Two magnets

Fig. 2 Magnet arrangements

3. RESULTS AND DISCUSSION

3.1 Validation Trial

The validation trial was carried out without a magnetic field. **Fig. 3** shows the local Nusselt number Nu_x versus local modified Rayleigh number Ra_x^* without such a field.

In the figure, our experimental values are compared with those obtained from the Nu_x-Ra^*_x relation of a single vertical heated plate in Ref.[21], which is

$$Nu_x = \left\{ \frac{\Pr_\infty}{4 + 9\Pr_\infty^{1/2} + 10\Pr_\infty} \right\}^{\frac{1}{5}} \left(\frac{\nu_\infty}{\nu_w} \right)^{0.17} Ra_x^{*\frac{1}{5}} \quad (Ra_x^* < 10^{12} - 4 \times 10^{13}), \tag{19}$$

where the Prandtl number, $\Pr_\infty$, is 13.2 (at 292K) as obtained by the linear approximation of physical properties between water and $[Gd(NO_3)_3]_{aq}$ by Kenjereš, et al. [14] at our concentration.

As shown in the figure, the local Nusselt number in our study is smaller than in the reference data. This is probably due to the presence of the facing wall and the size of the flow domain (bath). The facing and side walls were to block the flow from the bulk region. These walls were mounted so that the upward flow was introduced vertically from the bottom of the duct [22]. Since the bath size was limited in our experiment, wall friction was possible along the bath and facing walls. Wall friction may reduce the local heat transfer coefficient. However, the slope of the Nu-Ra* line agrees with the reference data, which supports the validity of this experiment.
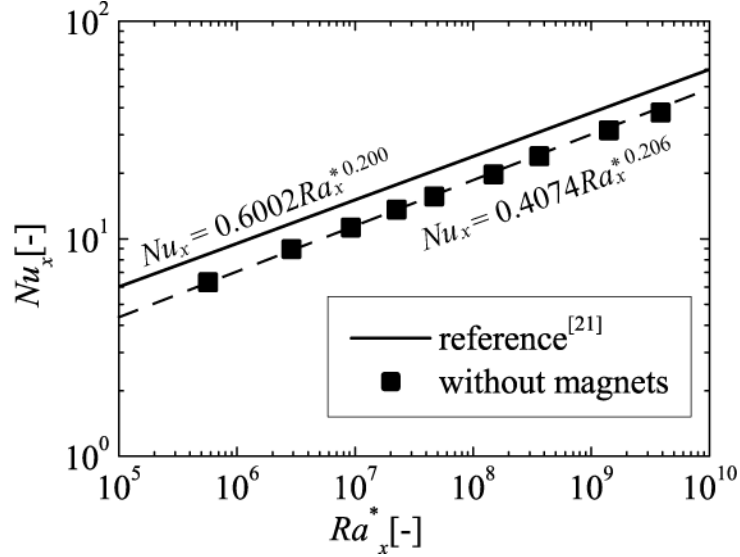
Fig. 3 Local Nusselt number versus modified Rayleigh number without magnetic field.

3.2 Effect of a Single Magnet on the Local Heat Transfer Coefficient

The first experiment was with a single magnet. The experimental positions are shown in **Fig. 4**. The cross-sectional size of the magnet was 10 mm × 10 mm, and three magnet elevations were examined. The magnet elevations were (a) from $x = -10$ mm to 0 mm (below the thermal developing region), (b) $x = 0$ mm to 10 mm (in the thermal developing region), and (c) $x = 60$ mm to 70 mm (settled in the thermally developed region). According to Ref. [24]., the effect of the magnetic field on a pipe flow becomes remarkable when the magnet is placed at the inlet of heating region. The specific magnet locations in this study are based on the study.
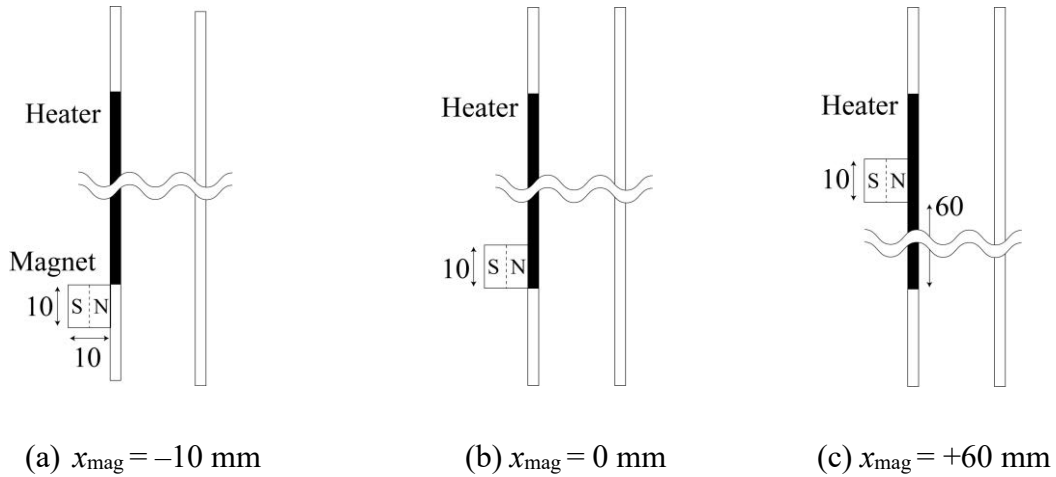

(a) $x_{mag} = -10$ mm   (b) $x_{mag} = 0$ mm   (c) $x_{mag} = +60$ mm

Fig. 4 Elevation of the single magnet.

The steady-state local heat transfer coefficient is summarized in **Fig. 5** with and without the magnet. The abscissa represents the distance from the bottom of the heated wall. We found that the effect of the magnetic force on the natural convection depended on the magnet elevation. In **Fig. 5(a)**, the local heat transfer coefficient is enhanced

for 0 mm $< x <$ 10 mm. When the magnet is raised by 10 mm, the heat transfer is suppressed and then enhanced for 0 mm $< x <$ 20 mm. In both cases, the local heat transfer coefficient away from the magnet coincides with that without the magnetic field. When the magnet is away from the thermally developing region, there is no significant effect (**Fig. 5(c)**). The effect is re-scaled as the ratio between with and without magnet in **Fig. 6** for the reference.

These facts suggest that when the magnet is placed behind the heater, the magnetic force from the upper edge of the magnet enhances the convection, and that from the lower magnet edge suppresses the heat transfer. These effects are significant when the magnet is in the developing region of the thermal boundary. This tendency was observed in forced convection in a pipe [24]. In that study, the magnetic field was produced by a single-turn electric coil, thus the thickness of the magnet was negligible. In our experiment we found that the magnetic force at magnet edges dominated the effect on natural convection.
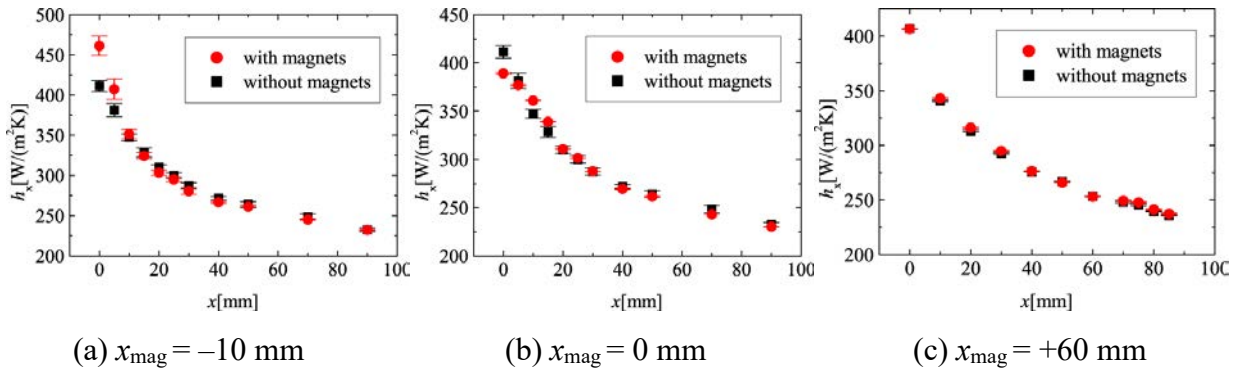

(a) $x_{mag} = -10$ mm (b) $x_{mag} = 0$ mm (c) $x_{mag} = +60$ mm
Fig. 5 Local heat transfer coefficient along the heated wall with/without magnet.

(a) $x_{mag} = -10$ mm (b) $x_{mag} = 0$ mm (c) $x_{mag} = +60$ mm
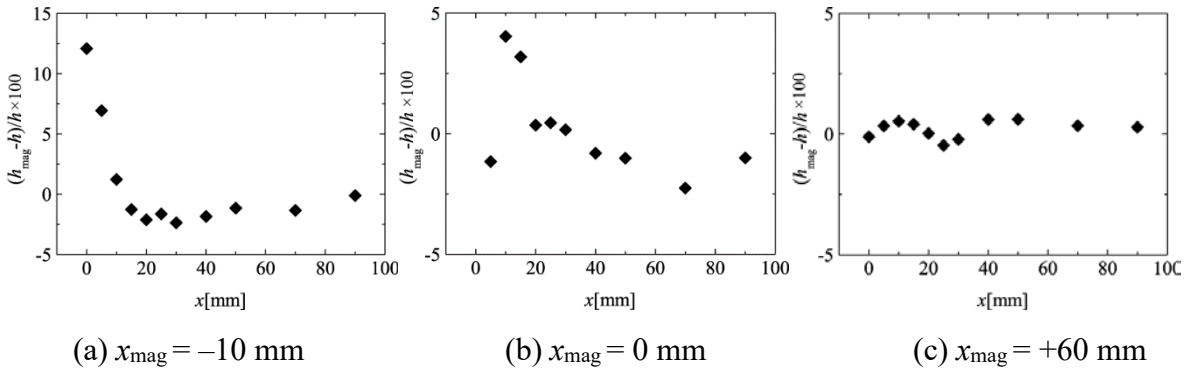**Fig. 6** Ratio of local heat transfer enhancement/suppression by magnet.

3.3 Magnetic Force by a Single Magnet

Fig. 7 shows the two-dimensional magnetic field pattern and the gradient of the squared magnetic induction for a single magnet. The size of the magnet and surface magnetic induction correspond to those of our experiment (10 mm × 10 mm and 573 mT). As **Fig. 7(a)** shows, the magnetic field is symmetric. The vector data in **Fig. 7(b)** are drawn in the region of the fluid, which is the magnetic force as shown in Eq. (1). As shown in the figure, the magnetic force becomes significant near the top and bottom magnet edges.
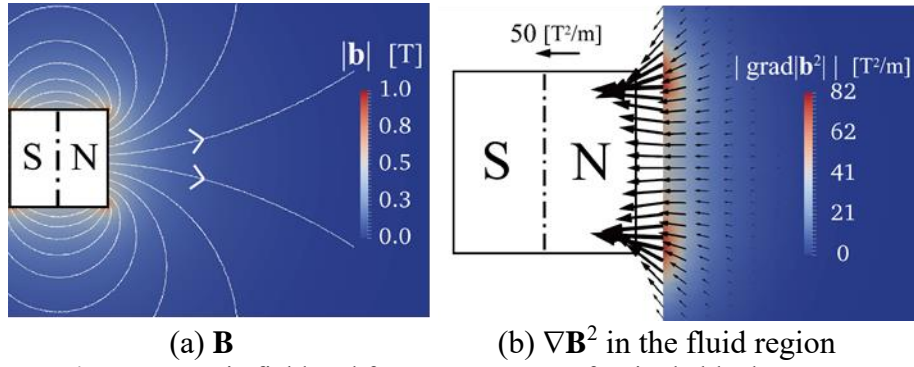
(a) **B**   (b) $\nabla \mathbf{B}^2$ in the fluid region

Fig. 7 Magnetic field and force component of a single block magnet.

In the absence of buoyancy, meaning the fluid near the magnet is not heated, the fluid experiences a magnetic force corresponding to that of **Fig. 7(b)** in addition to gravitational force. Since the magnetic force is diagonally upward/downward toward the bottom/top magnet edge, the resultant force becomes asymmetric as illustrated in **Fig. 8**. The magnetic force adds together with gravity near the top magnet edge and partially cancels it near the bottom edge.

When the magnet is behind the heated region, buoyant force is induced if the fluid temperature is higher than that of the surrounding. Since both the magnetic and gravitational forces depend on the fluid density, the buoyancy is against the gravitational and magnetic forces as shown in **Fig. 8**, which is called the magnetothermal force.
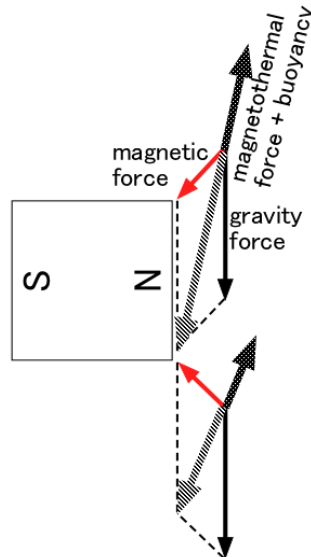

Fig. 8 Schematic of resultant of magnetic, gravitational, and buoyant (magnetothermal) forces by a single block magnet.

Therefore, the effect of the magnetic field shown in **Fig. 5** can be explained as follows. In **Fig. 5(a)**, the buoyancy, aided by the magnetic force, is induced near the top magnet edge, and the gravitational force is partly cancelled near the bottom magnet edge. These work to accelerate the upward natural convection, and the local heat transfer

coefficient is enhanced above the magnet. In **Fig. 5(b)**, buoyancy near the top magnet edge is enhanced due to higher temperature. It is also induced near the bottom magnet edge, which is partly cancelled by the magnetic force. Therefore, the natural convection is suppressed near the bottom edge. As the magnet elevation increases (**Fig. 5(c)**), the buoyant force against the resultant force of magnetic and gravity becomes stronger according to the definition. However, the effect is canceled probably due to the presence of both enhancement and suppression effects in the confined duct. This should be further discussed by numerical simulation.

3.4 Effect of the Magnetic Field of Multiple Magnets

We found that the effect of the magnetic force depends on the relative locations of the magnet and heated plate. If the magnitude of $\nabla \mathbf{B}^2$ is increased by arranging multiple magnets, the effect can be enhanced. The arrangement of **Fig. 2(b)** was used and measurements were made. The locations of two alternating-pole magnets are shown in **Fig. 9**.
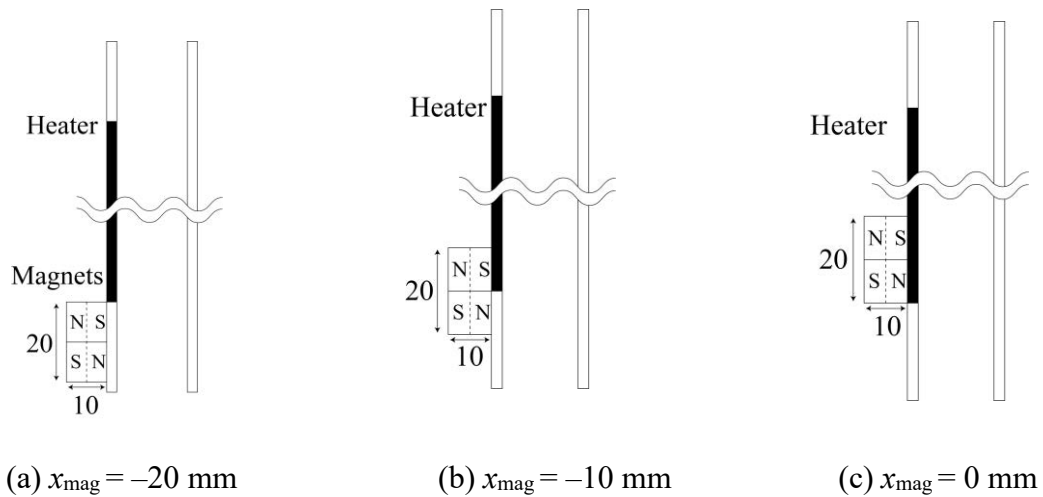

(a) $x_{mag} = -20$ mm   (b) $x_{mag} = -10$ mm   (c) $x_{mag} = 0$ mm
Fig. 9 Elevation of two alternating-pole magnets.

The magnetic field and $\nabla \mathbf{B}^2$ are shown in **Fig. 10**. The vector scaling of **Fig. 10(b)** is the same as in **Fig. 7(b)**. As expected, the magnetic force is strongest at the junction between the two magnets. It is also interesting that the force is directed horizontally toward the junction.
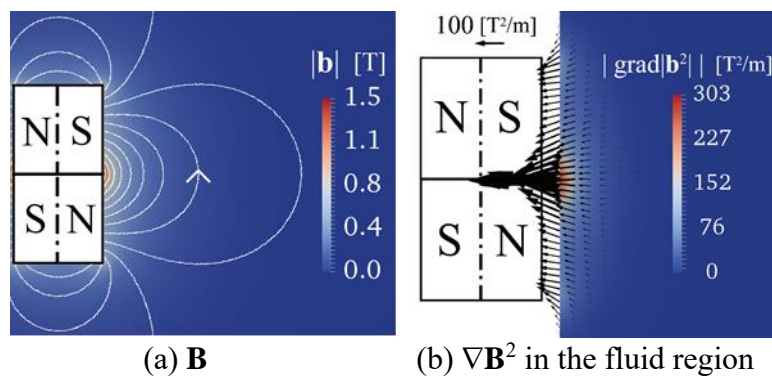

(a) **B**   (b) $\nabla \mathbf{B}^2$ in the fluid region
Fig. 10 Magnetic field and magnetic force of two block magnets.

The resulting local heat transfer coefficient is shown in **Fig. 11**. The effect in **Fig. 11(a)** is similar to that in **Fig. 5**. This suggests that the magnetic force near the bottom of the heater is the main factor enhancing the heat transfer rather than the force near the magnet junction. When the magnets are raised by 10 mm (**Fig. 11(b)**), the magnet junction corresponds to the heater bottom. In this case, the local heat transfer is enhanced from the junction to $x =$ 20 mm. Its peak is at around $x = 5$ mm. This unique local heat transfer curve can be explained as follows. Around the magnet junction, $\nabla \mathbf{B}^2$ is symmetric along the junction line. If the heated fluid spreads on the right side of the junction, the heat transfer is enhanced above the junction and suppressed below it. The result shows that the effect of the magnetic force may be canceled by this enhancement and suppression near the magnet junction. As for the fluid above the junction, the magnetic force gradually enhances the convection, thus the local heat transfer coefficient increases until it merges with that of the zero-magnetic-field case. When the bottom edge of the lower magnet is at the same elevation as the heater bottom (**Fig. 11(c)**), the magnet junction is at $x = 10$ mm. In this case, since both magnets are behind the heated wall, the heat transfer is suppressed below the junction and then enhanced above it by the mechanism found in the single-magnet case. This also implies that the fluid just below the magnet junction is slightly heated, and the local magnetic force works to decrease the local heat transfer as suggested in **Fig. 11(b)**. The ratio of enhancement/suppression in the case is summarized in **Fig. 12**.

Consequently, although the magnitude of $\nabla \mathbf{B}^2$ increases from aligning two magnets with alternating poles, we find that the effect on the heat transfer along the heated wall is on the same order as that of the single magnet. However, this magnet arrangement has the potential to extend the effect of the magnetic force, as evident from the local magnetic force schematically shown in **Fig. 14**.
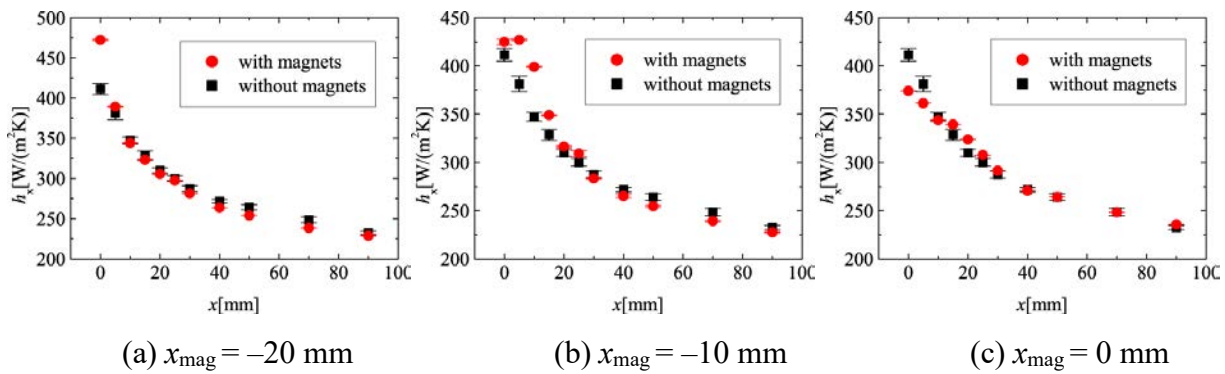

(a) $x_{\text{mag}} = -20$ mm   (b) $x_{\text{mag}} = -10$ mm   (c) $x_{\text{mag}} = 0$ mm

Fig. 11 Local heat transfer coefficient along the heated wall with/without two magnets.

(a) $x_{\text{mag}} = -20$ mm   (b) $x_{\text{mag}} = -10$ mm   (c) $x_{\text{mag}} = 0$ mm
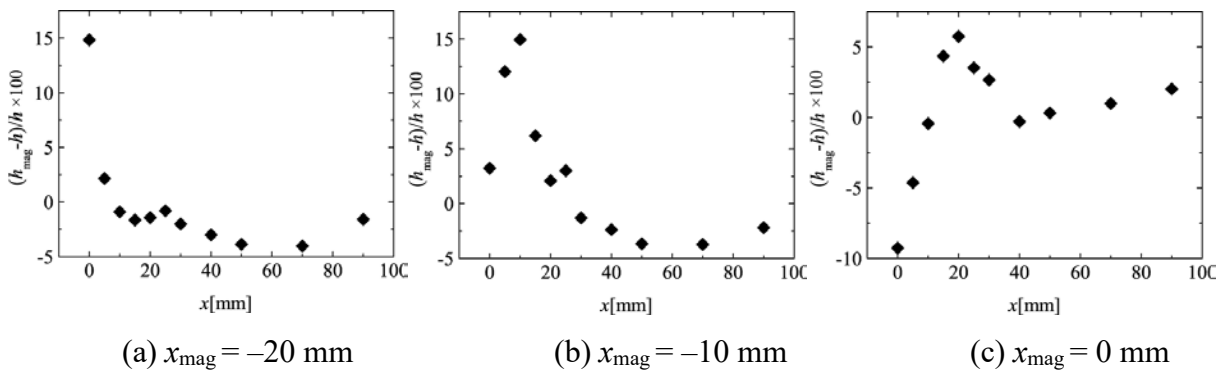
Fig. 12 Ratio of local heat transfer enhancement/suppression by magnet by two magnets.
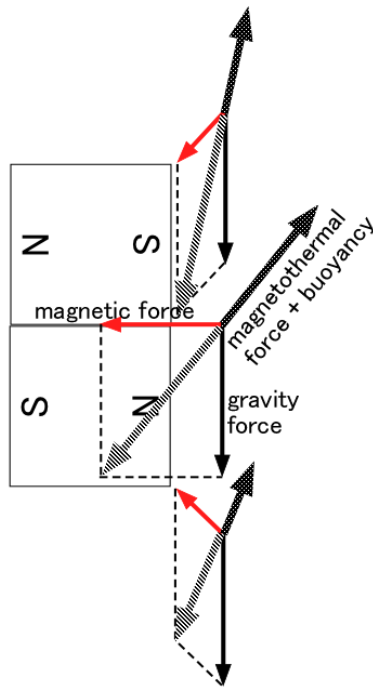
11

Fig. 13 Schematic of gravitational, magnetic, and buoyant forces for two magnets.

4. CONCLUSION

We have studied the effect of magnetic fields on natural convection of a paramagnetic liquid in a partially-heated vertical duct. For a single permanent magnet, the local heat transfer coefficient becomes large when the magnet upper side is on the bottom end of the heater. This suggests that the magnetic field near the top of the magnet enhances the natural convection heat transfer. Raising the elevation of the magnet suppresses the effect around its bottom edge when buoyancy acts on the fluid. These effects become weak as the magnet is placed much higher along the heated wall. These findings can be explained by the action of buoyancy against the resultant of gravitational and magnetic forces.

We have also found that pairing two magnets with their poles aligned and alternating enhances the magnetic force especially at the magnet junction. The influence of the magnetic field can be understood as a combination of effects at the magnet junction, upper edge of the upper magnet, and lower edge of the lower magnet.

This study has shown that a permanent magnet affects the natural convection of paramagnetic liquid, and that this effect can be enhanced by using multiple magnets.

REFERENCES

[1] Faraday, M., "On the diamagnetic conditions of flame and gases," *The London, Edinburgh, and Dublin Philosophical Magazine and Journal of Science*, **XXXI**, third ser., pp. 401-421, (1847).

[2] L. Pauling, R.E. Wood, J. H. Sturdivant, An instrument for determining the partial pressure of oxygen in a gas, Journal of the American Chemical Society, 68, 795-798, 1946.

[3] A.R. Carruthers, R. Wolfe, Magnetothermal convection in insulating paramagnetic fluids, Journal of Applied Physics, 39, 5718-5722, 1968.

[4] D. Melville, F. Paul, S. Roath, Direct magnetic separation of red cells from whole blood, Nature, 255, 706, 1975.

[5] M. Fujiwara, E. Oki, M. Hamada, Y. Tanimoto, I. Mukouda, and Y. Shimomura, Magnetic Orientation and Magnetic Properties of a Single Carbon Nanotube, Journal of Physical Chemistry, 105,18, 4383-4386, 2001.

[6] Y-Z Guo, D-C Yin *, H-L Cao, J-Y Shi, C-Y Zhang, Y-M Liu, H-H Huang, Y. Liu, Y. Wang, W-H Guo, A-R Qian and P. Shang, Evaporation Rate of Water as a Function of a Magnetic Field and Field Gradient, Int. J. Molecular Sciences, 13, 16916-16928, 2012.

[7] K. Kitazawa, Y. Ikezoe, H. Uetake, N. Hirota, "Magnetic field effects on water, air and powders," *Physica B*, **294-295**, pp. 709-714, (2001).

[8] Wakayama, N.I., "Behavior of gas flow under gradient magnetic fields," *J. Appl. Phys.*, **69**, 2734, (1991).

[9] Bai, B., Yabe. A., Qi, J., Wakayama, N.I., "Quantitative analysis of air convection caused by magnetic-fluid coupling", *AIAA Journal*, **37**(12), pp. 1538-1543, (1999).

[10] Uetake, H., Hirota, N., Nakagawa, J., Ikezoe, Y., Kitazawa, K., "Thermal Convection Control by Gradient Magnetic Field," *J. Appl. Phys.*, **87**(9), pp. 6310-6312, (2000).

[11] Braithwaite, D., Beaugnon, E., Tourniew, R., "Magnetically controlled convection in a paramagnetic fluid," *Nature*, **354**(14), pp. 134-136, (1991).

[12] Akamatsu, M., Higano, M., Takahashi, Y., Ozoe, H., "Numerical computation of magnetothermal convection of water in a vertical cylindrical enclosure," *Int. J., Heat Fluid Flow*, **26**, pp. 622-634, (2005).

[13] Kenjereš, S., Pyrda, L., Wrobel, W., Fornalik-Wajs, E., Szmyd, J.S., "Oscillatory states in thermal convection of a paramagnetic fluid in a cubical enclosure subjected to a magnetic field gradient," *Phys. Rev. E.*, **85**, 046312, (2012).

[14] Kenjereš, S., Pyrda, L., Fornalik-Wajs, E., Szmyd, J.S., "Numerical and experimental study of Rayleigh-Benard-Kelvin convection," *Flow Turbulence Combust.*, **92**, pp. 371-393, (2014).

[15] Maki S., Ataka M., Tagawa T., Ozoe H., Mori W., "Natural convection of a paramagnetic liquid controlled by magnetization force," *AIChE Journal*, **51**, pp. 1096-1103, (2005).

[16] A. Ujihara, T. Tagawa, H. Ozoe, Average heat transfer rates measured in two different temperature ranges for magnetic convection of horizontal water layer heated from below, *Int. J. Heat Mass Trans.*, 49, 3555-3560, 2006.

[17] R. Shigemitsu, T. Tagawa, H. Ozoe, Numerical computation for natural convection of air in a cubic enclosure under combination of magnetizing and gravitational forces, Numerical Heat Transfer, Part A, 43, 5 , 449-463, 2003.

[18] W.A. Wrobel, E. Fornalik-Wajs, J.S. Szmyd, Analysis of the influence of a strong magnetic field gradient on convection process of paramagnetic fluid in the annulus between horizontal concentric cylinders, Journal of Physics: Conference Series, 395, 012124, 2012.

[19] S. Maki, Y. Oda, M. Ataka, High-quality crystallization of lysozyme by magneto-Archimedes levitation in a superconducting magnet, Journal of Crystal Growth, 261, 557-565, 2004.

[20] H. Ozoe, S.W. Churchill, Hydrodynamic stability and natural convection in Newtonian and non-Newtonian fluids heated from below, AIChE Symposium Series, Heat Transfer 69 (131) (1973) 126‑133.

[21] T. Fujii, M. Fujii, The dependence of local Nusselt number on Prandtl number in the case of free convection along a vertical surface with uniform heat flux, *Int. J. Heat Mass Trans.*, 19, 121-122, 1976.

[22] Fujii, T., Saito, A., Katayama, K., Hattori, K., Toda, S., Progress in heat transfer: Yokendo, (1974) (in Japanese).

[23] Kenjereš, S., "Electromagnetically driven dwarf tornados in turbulent convection", Phys. Fluids, 23, 015103, 2011.

[24] M. Kaneda, K. Suga, Magnetothermal force on heated or cooled pipe flow, International Journal of Heat and Fluid Flow, 69, pp. 1-8, 2018.